Characterization of a New Humanized Anti-CD20 Monoclonal Antibody, IMMU-106, and Its Use in Combination with the Humanized Anti-CD22 Antibody, Epratuzumab, for the Therapy of Non-Hodgkin's Lymphoma

Rhona Stein,[1] Zhengxing Qu,[2] Susan Chen,[1] Adriane Rosario,[1] Victoria Shi,[2] Marianne Hayes,[2] Ivan D. Horak,[2] Hans J. Hansen,[2] and David M. Goldenberg[1]

[1]Garden State Cancer Center, Center for Molecular Medicine and Immunology, Belleville, and [2]Immunomedics, Inc., Morris Plains, New Jersey

ABSTRACT

Purpose: **A new humanized anti-CD20 monoclonal antibody (MAb), IMMU-106, was evaluated to elucidate its action as an antilymphoma therapeutic, as a single agent, and in combination with the anti-CD22 MAb, epratuzumab.**

Experimental Design: **Antiproliferative effects, apoptotic effects, and the ability of IMMU-106 to mediate complement-mediated cytotoxicity and antibody-dependent cellular cytotoxicity on a panel of non-Hodgkin's lymphoma (NHL) cell lines were compared with the chimeric anti-CD20 MAb, rituximab, and evaluated in light of the various levels of antigen expression by the cell lines. *In vivo* therapy studies were performed in SCID mice bearing disseminated Raji lymphoma.**

Results: **The mechanisms of cytotoxicity of IMMU-106 were found to be similar to rituximab, and include direct apoptosis, antibody-dependent cellular cytotoxicity, and complement-mediated cytotoxicity. IMMU-106 was also found to be very similar to rituximab in terms of antigen-binding specificity, binding avidity, and dissociation constant. Treatment of Raji-bearing SCID mice with IMMU-106 yielded median survival increases of up to 4.2-fold compared with control mice. Survival in mice treated with IMMU-106 plus epratuzumab was compared with IMMU-106 treatment alone. Although the combined treatment did not improve median survival, an increased proportion of long-term survivors was observed. An enhanced antiproliferative effect was also observed *in vitro* in SU-DHL-6 cells when IMMU-106 was combined with epratuzumab. These findings are consistent with the up-regulation of CD22 expression observed after pretreatment of NHL cells *in vitro* with CD20 MAb (IMMU-106).**

Conclusions: **It is expected that in humans IMMU-106 should be at least as effective as rituximab and, due to its human framework construction, it may exhibit different pharmacokinetic, toxicity, and therapy profiles. In addition, it may be possible to enhance efficacy by combination therapy comprised of anti-CD20 and other B-cell lineage targeting MAbs, such as epratuzumab. The current results emphasize that *in vitro* as well as *in vivo* studies with many of the NHL cell lines were generally predictive of the known activity of anti-CD20 MAbs in NHL patients, as well as the enhanced efficacy of epratuzumab combined with rituximab observed in early clinical trials.**

INTRODUCTION

Pan-B-cell monoclonal antibodies (MAbs) have been demonstrated to be effective antilymphoma agents (1). Comparison of the relative merits of various anti-B-cell MAbs for therapy of B-cell malignancies has delineated the importance of several parameters in determining the ultimate efficacy of these agents, such as antigen density and the ability to induce complement-mediated cytotoxicity (CMC; Refs. 2–4), antibody-dependent cytotoxicity (ADCC; Ref. 5), and/or direct induction of apoptosis (6–8). It is likely that, depending on the system, more than one of these mechanisms plays a role in the effectiveness of a MAbs. It is also clear, however, that not all of the parameters have been elucidated, especially with regards to the properties that define which MAb would be a likely best choice across non-Hodgkin's lymphoma (NHL) subtypes and for individual cases within a subtype, as well as how to augment the efficacy of naked MAbs by combination with other treatment modalities.

The chimeric anti-CD20 antibody, rituximab (Rituxan; Genentech, South San Francisco, CA; IDEC, San Diego, CA), has been approved for the treatment of relapsed/refractory low-grade B-cell non-Hodgkin's lymphoma (9). Whereas rituximab is effective, only ~50% of patients respond when given 375 mg/m^2 weekly for 4 weeks (9). The median time to progression in responders is ~13 months (9), and ~60% of initial responders do not respond to retreatment (10). Because of these limitations, as well as the long initial infusion time necessary for administration of rituximab and the occurrence of infusion-related toxicities (11), there is an ongoing effort for improvement in this treatment modality. Other antibodies under investigation as potential therapeutic agents for NHL include anti-CD19, -CD22, -CD52, -CD74, -CD80, and -HLA-DR MAbs (12–19). As with rituximab, it is unlikely that these MAbs will be curative as single agents. Combination therapy,

Received 10/29/03; revised 12/22/03; accepted 1/2/04.
Grant support: Immunomedics, Inc., Morris Plains, NJ.
The costs of publication of this article were defrayed in part by the payment of page charges. This article must therefore be hereby marked *advertisement* in accordance with 18 U.S.C. Section 1734 solely to indicate this fact.
Requests for reprints: Rhona Stein, Garden State Cancer Center, 520 Belleville Avenue, Belleville, NJ 07109. Phone: (973) 844-7012; Fax: (973) 844-7020; E-mail: rstein@gscancer.org.

for example, with chemotherapy or of multiple MAbs targeting antigens with different signaling pathways may be necessary. The rational design of combination MAb therapy will depend on knowledge of the precise mechanism of action of the MAbs, with improved results expected when agents to distinct targets, which function by nonoverlapping mechanisms, are combined. It is also conceivable that binding to one antigen target may affect the binding to, or expression of, another.

In this report, a new humanized anti-CD20 MAb, IMMU-106, was evaluated to elucidate its action as an antilymphoma therapeutic. The humanized anti-CD20 MAb, IMMU-106 (also known as hA20; Immunomedics, Inc., Morris Plains, NJ), was generated using the same human IgG framework as epratuzumab (Immunomedics, Inc.), a CDR-grafted (humanized) MAb directed against CD22 (20). Antiproliferative effects, apoptotic effects, and the ability of IMMU-106 to mediate complement-dependent cell lysis and ADCC of NHL cell lines are compared with the chimeric anti-CD20 MAb and rituximab, and evaluated in light of the various levels of antigen expression by the cell lines. The expression of CD20 and CD22 by NHL cells in culture was also examined after pretreatment with either CD22 or CD20 MAbs. The ability of the MAbs to prolong survival in an animal model of NHL is also demonstrated. In addition, enhancement of the *in vitro* and *in vivo* antitumor effects of the anti-CD20 MAb, IMMU-106, is shown when given in combination with epratuzumab.

MATERIALS AND METHODS

Cells

The Burkitt lymphoma lines, Daudi, Raji, and Ramos, were purchased from the American Type Culture Collection (Manassas, VA). Non-Burkitt lymphoma cell lines were obtained as follows. RL and SU-DHL-6, which contain the chromosomal translocation t(14;18), were obtained from Dr. John Gribben (Dana-Farber Cancer Institute, Boston, MA) and Dr. Alan Epstein (University of Southern California, Los Angeles, CA), respectively. Cell lines SU-DHL-4, SU-DHL-10, and Karpas422 were provided by Dr. Myron Czuczman (Roswell Park Cancer Institute, Buffalo, NY), and WSU-FSCCL and DoHH2 cell lines were obtained from Dr. Mitchell Smith (Fox Chase Cancer Center, Philadelphia, PA). The cells were grown as suspension cultures in DMEM (Life Technologies, Inc. Gaithersburg, MD), supplemented with 10% fetal bovine serum, penicillin (100 units/ml), streptomycin (100 μg/ml), and L-glutamine (2 mM; complete media).

Antibodies

Development of hLL2, the humanized anti-CD22 MAb, now referred to as epratuzumab, has been described previously (20, 21). Similar procedures were adopted to develop the humanized anti-CD20 MAb, designated as IMMU-106, or hA20. Briefly, the V_κ and V_H genes of the parent anti-CD20 MAb were first cloned from the hybridoma cells by reverse transcription-PCR, and the complementary determining region sequences were elucidated by DNA sequencing, as described (22). The V genes of complementary determining region-grafted (or humanized) anti-CD20 MAbs were then designed and engineered. The same human framework regions (FRs) used for derivation of epratuzumab were applied, *i.e.,* the FR1, 2, and 3 of EU and the FR4 of NEWM heavy chain served as the scaffold for V_H, and the REI FRs as the scaffold for V_κ. IMMU-106 was expressed in Sp2/0-Ag14 cells (American Type Culture Collection). A high-level IMMU-106-producing clone was developed as described (21). Both epratuzumab and IMMU-106 were produced in bioreactors and purified by a combination of affinity chromatography on Protein A columns and gel filtration on SE columns under GMP compliance.

Other MAbs used in the studies were rituximab, purchased from IDEC Pharmaceuticals Corp. (San Diego, CA), and hMN-14, or labetuzumab (humanized anticarcinoembryonic antigen IgG_1), provided by Immunomedics, Inc. The construction and characterization of hMN-14, used here as a negative isotype control, have been described previously (23).

Cell Surface Antigen-Binding Assays

A competitive binding assay was used to evaluate the antigen-binding specificity of the anti-CD20 MAbs. A constant amount (100,000 cpm; ~10 μCi/μg) of ^{125}I-labeled rituximab was incubated with Raji cells in the presence of various concentrations (0.2–700 nM) of IMMU-106 or rituximab at 4°C for 1–2 h. Unbound MAbs were removed by washing the cells in PBS. The radioactivity associated with cells was determined after washing. The maximum number of binding sites per cell and the apparent antigen-binding affinity constant of the anti-CD20 MAbs were determined by direct cell surface saturation binding of the radiolabeled MAbs and Scatchard plot analysis, as described by Trucco *et al.* (24), and Lindmo *et al.* (25). MAbs were labeled with ^{125}I by the chloramine-T method (26). The data shown are specific binding. Each experiment was done with two sets of cells: (*a*) cells preincubated with respective cold MAb to block all of the binding sites; and (*b*) cells preincubated with medium. After preincubation, the cells were aliquoted, and radiolabeled MAb at various concentrations was added. The counts from set 1 were considered as nonspecific binding and that from set 2 total binding. Specific binding is total binding − nonspecific binding.

Flow Cytometric Assays

Immunophenotyping. Indirect immunofluorescence assays were performed with the panel of cell lines described above, using FITC-goat antimouse IgG (Tago, Inc., Burlingame, CA) essentially as described previously (27) and analyzed by flow cytometry using a FACSCalibur (Becton Dickinson, San Jose, CA).

Analysis of Apoptosis. Flow cytometric analysis of cellular DNA was performed after propidium iodide staining (6, 28). NHL cells were placed in 24-well plates (5×10^5 cells/well) and subsequently treated with MAbs (5 μg/ml). Three wells were prepared with each MAb to study the effects of cross-linking with goat antimouse or goat antihuman second antibodies. After a 20-min incubation with the primary MAbs (37°C; 5% CO_2), $F(ab')_2$ goat antimouse IgG Fcγ-specific second antibody (The Jackson Laboratory, West Grove, PA) was added to one well from each primary MAb to adjust the second antibody concentration to 20 μg/ml. $F(ab')_2$ goat antihuman IgG Fcγ-specific (The Jackson Laboratory) was similarly added to

the second well from each primary MAb, and the volume of the third set was equalized by addition of medium. After a 48-h incubation (37°C; 5% CO_2), cells were transferred to test tubes, washed with PBS, and then resuspended in hypotonic propidium iodide solution (50 mg/ml propidium iodide in 0.1% sodium citrate; 0.1% Triton X-100). Samples were analyzed by flow cytometry using a FACSCalibur. Percentage of apoptotic cells was defined as the percentage of cells with DNA staining before G_1/G_0 peak (hypodiploid).

Up-Regulation of Antigen Expression. To assess the effects of preincubation of NHL cells with IMMU-106 or epratuzumab, cells were stained with FITC-labeled anti-CD20 and -CD22 MAbs after overnight incubation with the unlabeled MAbs. Briefly, 1×10^6 cells were incubated in 2.0 ml of complete medium, or complete medium containing 10 μg/ml of IMMU-106 or epratuzumab, in triplicate, in 24-well plates. After a 17-h incubation (37°C; 5% CO_2), cells were transferred to test tubes, washed with PBS and 1% BSA, and then resuspended in 350 μl PBS and 1% BSA. An aliquot (100 μl) from each incubation mixture was incubated with either FITC-CD8 (Becton Dickinson: anti-Leu-2a-FITC; molar ratio FITC:protein = 4:9) as a negative control, FITC-anti-CD20 (Beckman Coulter: B1-FITC; molar ratio FITC:protein = 5:10), or FITC-anti-CD22 (Caltag: RFB4-FITC; molar ratio FITC:protein = 6.07), according to the manufacturer's directions, for 30 min, then washed with PBS and 1% BSA, resuspended in 1% formalin, and analyzed by flow cytometry with the Becton Dickinson FACSCalibur.

Cytotoxicity Assays

Standard ^{51}Cr release assays were performed for the measurement of ADCC and CMC essentially as described (29). All of the assays were performed in triplicate. Blood specimens used in these studies were collected under a protocol approved by the Institutional Review Board. Normal human serum complement was purchased from Quidel Corporation (San Diego, CA). For the CMC assay, 25 μl of 1:5 dilution was added, followed by a 3-h incubation. For the ADCC, E:T cell ratios of ~50:1 were used, and incubations were for 4 h. All of the blood donors gave voluntary, written informed consent.

Percentage of specific lysis was calculated according to the following formula:

% lysis = [^{51}Cr release from experimental sample − spontaneous^{51}Cr release]/[^{51}Cr release from maximum release − spontaneous ^{51}Cr] × 100.

In Vitro Cell Proliferation Assays

Effects of MAbs, with or without Second Antibody Cross-Linking on [^{3}H]Thymidine Uptake. MAb effects on cell growth were determined by assessing [^{3}H]thymidine incorporation in the NHL cell lines with and without the presence of a cross-linking second antibody, essentially as described by Shan *et al.* (6). Second antibodies used for evaluating the effects of cross-linking were $F(ab')_2$ goat antimouse IgG Fcγ-specific or $F(ab')_2$ goat antihuman IgG Fcγ-specific (The Jackson Laboratory). All of the tests were performed in triplicate.

In Vivo Effects of Naked MAbs on SCID Mice Bearing Disseminated Raji

Mice were injected i.v. with $1–2.5 \times 10^6$ Raji cells on day 0. Administration of MAbs was initiated 1 day after injection of tumor cells according to dose schedules described for each experiment. Mice were examined daily for signs of distress or hind-leg paralysis and weighed weekly. Paralysis of the hind legs or weight loss of >25% was used as the survival end point. Animals were euthanized at these end points. Animal studies were performed under protocols approved by the Institutional Animal Care and Use Committee.

RESULTS

Antigen-Binding Characteristics of IMMU-106. IMMU-106 was designed to have human IgG1/κ constant regions and the same human V FRs as the humanized anti-CD22 antibody, epratuzumab. The antigen-binding specificity and affinity of IMMU-106 were evaluated by cell-surface competitive and direct saturation-binding assays, and compared with rituximab, a human-mouse chimeric anti-CD20 MAb. In the competitive binding assay, various concentrations of IMMU-106 or rituximab were used to compete with radioiodinated rituximab for the binding to Raji human NHL cells. The results shown in Fig. 1*A* confirmed that IMMU-106 has the same antigen-binding specificity as rituximab and the apparent binding avidities are comparable between these MAbs. This was additionally confirmed by direct cell surface saturation binding and Scatchard plot analysis to measure the dissociation constant of IMMU-106. As shown in Fig. 1*B*, the apparent dissociation constant values for IMMU-106 and rituximab were virtually the same, calculated to be 3.6 ± 0.6 and 3.1 ± 0.4 nM, respectively. Similar results were obtained on Daudi cells (data not shown).

Antigen Expression of Cultured Lymphoma Cell Lines and Normal Peripheral Blood Lymphocytes. Flow cytometry analysis was performed using indirect immunofluorescent staining to show that IMMU-106 binds to a panel of cultured B-cell lymphomas. As shown in Table 1, the MAb binds to all of the tested cell lines, but the level of fluorescence staining varied between the cell lines. IMMU-106 behaves similarly to rituximab, staining the Burkitt cell lines, Raji, Ramos, and Daudi, and the non-Burkitt (follicular and diffuse large B-cell lymphoma) lines, SU-DHL-6, RL, and DoHH2, with high intensity. Four other NHL lines, WSU-FSCCL, Karpas422, SU-DHL-4, and SU-DHL-10, exhibited lower levels of MAb staining. SU-DHL-6 had the highest staining intensity, followed by Raji. Examples of histograms representing 3 levels of staining intensity are shown in Fig. 2 for the SU-DHL-4, Raji, and SU-DHL-6 cell lines. The mean fluorescence intensity of IMMU-106 staining averaged 78% (range, 56–95%) of the rituximab levels. It is possible that this difference reflects a difference in the binding of the FITC-labeled second antibody (goat antihuman IgG) to the chimeric (rituximab) and humanized (IMMU-106) MAbs. This is supported by the observation that a human-mouse chimeric version of IMMU-106 yielded equivalent results to rituximab (mean percentage of rituximab value = 102%; range, 90–116%; data not shown).

MAb binding to normal human peripheral blood leukocytes also was assessed. Lymphocytes, monocytes, and granulocytes

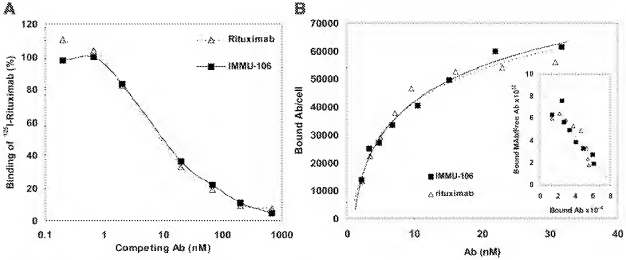

Fig. 1 Binding characteristics of IMMU-106. *A*, competitive binding assay. A cell surface competitive binding assay was performed to compare the binding activity of IMMU-106 with that of rituximab. Varying concentrations of IMMU-106 (■) or rituximab (△) were mixed with a constant amount of ^{125}I-rituximab and incubated with Raji cells at 4°C for 1 h. The cells were washed to remove unbound monoclonal antibodies and counted for the bound residual radioactivity. *B*, direct cell surface saturation binding and Scatchard plot analysis. IMMU-106, ■; rituximab, △; *Ab*, antibody.

were incubated with the anti-CD20 MAbs, followed by staining with FITC-labeled goat antihuman second antibody. Flow cytometry analysis indicated that staining of normal peripheral blood lymphocytes was similar for IMMU-106 and rituximab (Table 2). Positive staining was ~9% above the background with the anti-CD20 MAbs, which is within the normal range for percentage of B cells. Monocytes and granulocytes were negative.

Effects of Naked MAbs on Proliferation of NHL Cell Lines. Growth inhibition by the anti-B-cell MAbs was evaluated by *in vitro* proliferation assays in the NHL cell lines. Cells were cultured with the MAbs in solution with or without a second MAb for cross-linking, to mimic the role of effector cells *in vivo*. Proliferation was assessed by measuring the uptake of [^{3}H]thymidine. Controls included rituximab, no first MAb, and a negative control MAb, hMN-14. In all of the B-cell lines studied, specific inhibition was seen with the anti-CD20 MAbs, but the level of inhibition varied between the cell lines. As shown in Fig. 3, anti-CD20 MAbs yielded specific inhibition of proliferation in the Burkitt and non-Burkitt lymphoma cell lines. However, inhibition of proliferation was not directly related to antigen density. For example, CD20 expression is greater in Raji than Daudi, yet inhibition of proliferation of Daudi cells by anti-CD20 MAbs was greater than that of Raji cells. In the Raji experiment, inhibition of proliferation by the anti-CD20 MAbs was ~20% and with cross-linking ~40%, compared with Daudi in which >60% inhibition was seen with cross-linked anti-CD20 MAbs, IMMU-106, and rituximab. Among the non-Burkitt lymphoma cell lines, SU-DHL-6 was markedly more sensitive to antiproliferative effects of the MAbs than RL, SU-DHL-4, and SU-DHL-10, as well as the Burkitt lines. In the absence of cross-linking, IMMU-106 and rituximab yielded ~88% inhibition of proliferation of SU-DHL-6 cells, and with cross-linking specific inhibition of proliferation increased to 98%. Results with these cell lines again indicate that inhibition of proliferation is not directly related to antigen density. Whereas CD20 expression is in the order SU-DHL-6 > RL > Raji > Daudi, sensitivity of proliferation to anti-CD20 MAbs is in the order SU-DHL-6 > Daudi > Raji > RL. SU-DHL-4 and SU-DHL-10 express low levels of CD20 and are relatively insensitive to the anti-CD20 MAbs (data not shown).

Mechanistic Studies. Apoptosis, ADCC, and CMC were evaluated using a panel of B-cell lymphoma cell lines.

Induction of Apoptosis by Naked MAbs in NHL Cell Lines. Induction of apoptosis was evaluated by flow cytometry assays on the B-cell line panel. Cells were cultured with the MAbs for 48 h with or without a second MAb for cross-linking, followed by DNA staining with propidium iodide. Cells were analyzed by flow cytometry, and positive florescence below the G_1 region represents DNA fragmentation and is a measure of apoptosis. Controls included rituximab, no first MAb, and the isotype negative control MAb, hMN-14. Results with SU-DHL-6 cells are shown in Fig. 4. In all of the B-cell lines studied, specific induction of apoptosis was seen with the anti-

Table 1 Antigen expression: indirect flow cytometry assay (geometric mean fluorescence)

	hMN-14	Rituximab	IMMU 106
Burkitt's			
Daudi	5.9	252.9	222.6
Raji	2.2	384.7	268.4
Ramos	1.1	119.5	82.6
Non-Burkitt's			
DoHH2	4.8	45.6	41.9
Karpas422	8.3	12.2	11.6
RL	3.1	158.9	130.8
SU-DHL-4	2.5	46.8	26.3
SU-DHL-6	1.6	599.5	439.2
SU-DHL-10	2.5	35.7	26.5
WSU-FSCCL	3.0	36.4	28.5

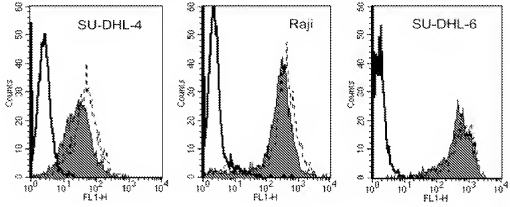

Fig. 2 Antigen expression on non-Hodgkin's lymphoma cell lines. Flow cytometry histograms are shown for three of the cell lines listed in Table 1. *Open solid line,* hMN-14; *filled solid line,* hA20; *dashed line,* rituximab.

Table 2 MAb[a] binding to peripheral blood lymphocytes

	Mean fluorescence	Percent positive
No first MAb	13	6.7
hMN-14	19	10.1
Rituximab	34	15.4
IMMU-106	30	15.6

[a] MAb, monoclonal antibody.

CD20 MAbs when an appropriate cross-linking agent was used. In the majority of cell lines apoptosis was not induced with any of the tested MAbs in the absence of cross-linking (Table 3). SU-DHL-6 is the exception; in this cell line the anti-CD20 MAbs also induced apoptosis without cross-linking.

ADCC and CMC. The ability of the anti-B-cell MAbs to induce ADCC and CMC was assayed using standard ^{51}Cr release assays and a homogeneous fluorometric lactate dehydrogenase release assay (Promega; data not shown). As measured by both methods, incubation of B-lymphoma cells with rituximab and IMMU-106 caused ADCC and CMC in the presence of human peripheral blood mononuclear cells or human complement, respectively (Figs. 5 and 6). Similar to the results observed in the proliferation and apoptosis evaluations, sensitivity of cell lines to ADCC varied, as noted by the *Y*-axis scales in Fig. 5. Levels of cytotoxicity were similar for rituximab and IMMU-106 in these studies.

***In Vivo* Effects of Naked MAbs on SCID Mice Bearing Disseminated Raji Lymphoma.** *In vivo* therapy studies were performed in SCID mice bearing systemic Raji tumors. Mice were injected i.v. with Raji cells on day-0. Fig. 7 shows a comparison of the anti-CD20 MAbs IMMU-106 and rituximab. MAbs were administered i.p. 5 times/week for 2 weeks, at 100 μg/injection, starting 1 day after injection of Raji cells, then twice weekly until day 36 of the study. Control mice received 100 μl of PBS, the MAb diluent, on each injection date. Control mice died of disseminated disease manifested with central nervous system paralysis, with a median survival time of 16.5 days

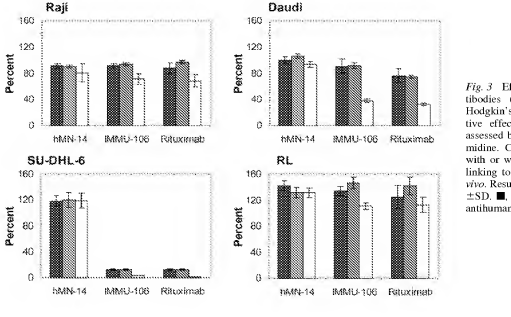

Fig. 3 Effects of anti-CD20 monoclonal antibodies (*MAbs*) on proliferation of non-Hodgkin's lymphoma cell lines. Antiproliferative effects of the anti-B-cell MAbs were assessed by measuring the uptake of [^{3}H]thymidine. Cells were cultured with the MAbs with or without a second antibody for cross-linking to mimic the role of effector cells *in vivo*. Results of four cell lines are shown; *bars,* ±SD. ■, no second Mab; ▨, antimouse; □, antihuman.

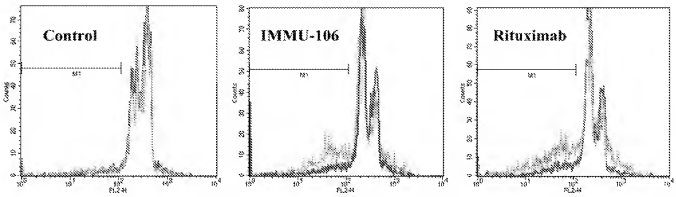

Fig. 4 Apoptotic effect of monoclonal antibodies on SU-DHL-6 cells. Induction of apoptosis was evaluated by flow cytometry determination of hypodiploid DNA on the B-cell line panel. Cells were cultured with the monoclonal antibodies without a second antibody (*purple line*), with goat antimouse IgG (*pink line*), or with goat antihuman IgG (*green line*), followed by DNA staining with propidium iodide. Results with SU-DHL-6 cells are shown. Hypodiploid DNA peaks corresponding to apoptotic nuclei were quantified in region M1.

after Raji tumor inoculation. Median survival in the treated groups was extended to 98 days for rituximab and 70 days for IMMU-106, statistically significant survival extensions in this model by log rank analysis ($P < 0.0001$). No statistical difference was observed between the effects of IMMU-106 and rituximab. These values represent median survival increases of 5.9-, and 4.2-fold for rituximab and IMMU-106, respectively, compared with control mice. Subsequent studies evaluated the importance of the Fc region for effective therapy by comparing the anti-CD20 MAbs, IMMU-106, and rituximab, and their $F(ab')_2$ fragments. The $F(ab')_2$ fragments were ineffective (data not shown), with identical median survival to control animals, confirming previous reports on the importance of Fc-mediated functions (CMC or ADCC).

Effects of Combining Anti-B-Cell MAbs. Combinations of MAbs recognizing distinct tumor-associated antigens can potentially enhance antitumor activity. To explore this possibility, the effects of combining IMMU-106 and epratuzumab were studied *in vitro* by evaluating effects on proliferation of cells in culture and *in vivo* in SCID mice bearing disseminated Raji tumors. As shown in Figs. 8 and 9, the combination of the two naked MAbs appears to be more effective than either agent alone.

Fig. 8 shows the results of an *in vitro* proliferation assay by [^{3}H]thymidine uptake. IMMU-106 alone caused a 53% inhibition of proliferation of SU-DHL-6 cells, and epratuzumab alone had no effect. The combination of the two agents increased inhibition of proliferation to 83% ($P < 0.001$, a significant difference from effect of IMMU-106 alone). This level of inhibition is similar to that obtained by cross-linking IMMU-106 with goat antihuman second antibody.

The survival curves shown in Fig. 9 represent combined data of two experiments comparing the effects of IMMU-106 given alone and in combination with epratuzumab. Each MAb was administered at 50 μg/injection, twice weekly, starting 1 day after tumor cell injection. In the combined MAb treatment group, each MAb was given twice weekly at 50 μg/injection. This dose is lower than that administered in the experiment shown in Fig. 7 and was selected to facilitate observation of improvements caused by the MAb combination. Median survival was 15 days in the untreated, isotype-matched control (hMN-14) and epratuzumab groups. IMMU-106 administered alone increased median survival to 25 days, and the combination of IMMU-106 and epratuzumab yielded a small increase in median survival; however, prolonged survival was observed in 30% of the mice. Day 35 was the time point at which the last animal reached the end point (hind-leg paralysis) in the IMMU-106-alone treatment group, whereas in the IMMU-106+epratuzumab group, 6 of 20 mice were still surviving at this time point. Survival in these 6 mice ranged from 43 to 72 days. Statistical significance of the effect was barely not reached *in vivo* ($P = 0.0515$ log rank test) for the difference between IMMU-106 and IMMU-106+epratuzumab.

Up-Regulation of CD22 by Anti-CD20. Mechanisms of enhancement of efficacy may include up-regulation of antigen levels as well as synergy between two different signaling pathways. Impact on receptor expression was examined by studying the CD22 and CD20 antigen density on cultured B-cell lines

Table 3 Apoptotic effect of anti-CD20 MAbs[a] as shown by propidium iodide staining (% hypodiploid DNA)

1st MAb/ 2nd MAb	SU-DHL-6			Daudi			RL		
	None	GAM	GAH	None	GAM	GAH	None	GAM	GAH
None	4.2	3.9	7.0	1.4	1.6	1.3	2.4	3.4	2.0
hMN-14	3.9	4.0	6.7	1.3	1.2	2.2	1.8	4.9	4.6
Rituximab	9.4	10.3	25.7	1.2	1.6	15.0	3.7	4.4	14.1
IMMU-106	10.6	9.3	29.5	1.5	1.5	14.6	3.4	2.7	25.1

[a] MAb, monoclonal antibody.

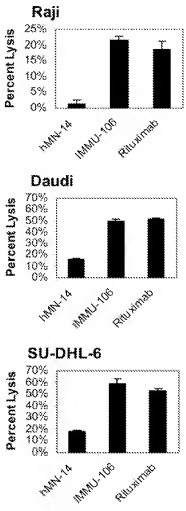

Fig. 5 Antibody-dependent cytotoxicity on non-Hodgkin's lymphoma cell lines. ^{51}Cr-labeled non-Hodgkin's lymphoma cells were incubated with anti-B-cell monoclonal antibodies in the presence of human peripheral blood mononuclear cells. The cells were incubated for 4 h at 37°C, followed by collection and counting of supernatants. Percentage of specific lysis of three cell lines is shown; *bars*, ±SD.

after incubation of the cells with epratuzumab or IMMU-106. Fig. 10 shows the flow cytometry histograms demonstrating that CD22 expression is up-regulated after overnight incubation with IMMU-106. As shown in Fig. 10, the histogram representing CD22 expression level after exposure to IMMU-106 is shifted to the right relative to the histogram representing CD22 expression with no prior exposure to IMMU-106. Mean fluorescent intensity increased from 21 to 28, an increase of 33%. Incubation of cells with epratuzumab did not increase the density of CD20 (data not shown).

DISCUSSION

Several issues must be considered to understand and try to improve upon the success of antibody-based treatments for NHL. The work reported herein addresses some of these issues. First, in an effort to improve upon the results obtained with rituximab, a humanized anti-CD20 MAb was developed by complementary determining region grafting. Rituximab is a murine-human chimeric MAb, in which the variable domains are derived from the murine anti-CD20 MAb, and the constant regions from human IgG1 heavy chain and human κ light chain. Although a chimeric antibody is less likely than a fully murine MAb to provoke an immune response, and elicitation of a human antichimeric antibody response has not posed a significant obstacle to the use of rituximab, it may be advantageous clinically to have a more fully human version, especially if repeated injections may be desired in patients, *e.g.*, for nonmalignant diseases, such as autoimmune diseases. Administration of humanized MAbs could possibly result in altered pharmacokinetic and toxicity profiles. A possible extension in serum half-life may permit extended dosing intervals and lead to reduced immunogenicity. Changes in pharmacokinetics and dosing regimens may affect the therapeutic response as well as toxicity. Although these benefits are theoretical at this time, remaining to be proven in clinical studies, such studies with

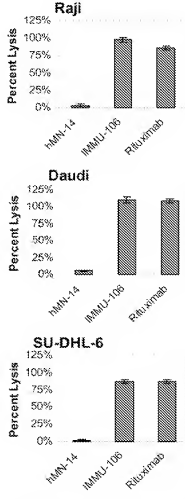

Fig. 6 Complement-mediated cytotoxicity on non-Hodgkin's lymphoma cell lines. ^{51}Cr-labeled non-Hodgkin's lymphoma cells were incubated with anti-B-cell monoclonal antibodies in the presence of human complement. The cells were incubated for 3 h at 37°C, followed by collection and counting of supernatants. Percentage of specific lysis of three cell lines is shown; *bars*, ±SD.

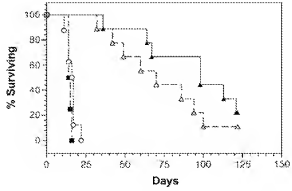

Fig. 7 Survival proportions in SCID mice bearing disseminated Raji cells; comparison of IMMU-106 and rituximab. Monoclonal antibodies were administered to SCID mice 5 times/week for 2 weeks, at 100 μg/injection, then twice weekly until day 36 of the study. Monoclonal antibody injections were initiated 1 day after i.v. injection of Raji cells. Each treatment group contained 10 mice. ○, untreated; –■–, hMN-14; –△–, IMMU-106; —▲—, Rituximab.

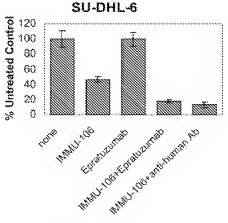

Fig. 8 Antiproliferative effects of the combination of IMMU-106 and epratuzumab by *in vitro* [^{3}H]thymidine uptake assay. SU-DHL-6 cells were cultured either without any added monoclonal antibody, or with IMMU-106, epratuzumab, the combination of IMMU-106 and epratuzumab, or the combination of IMMU-106 and goat antihuman IgG Fcγ-specific, for 48 h, followed by the addition of [^{3}H]thymidine and another 16-h incubation; *bars*, ±SD.

epratuzumab have demonstrated improved infusion properties, consisting of 30–60-min infusions (30) compared with infusion times of >4 h for rituximab (11). Epratuzumab administration has resulted in less infusion-related toxicity than has been evident with rituximab, and virtually no immune responses have been observed in patients given either the naked (30) or radioconjugated humanized epratuzumab, even when repeated, fractionated doses were administered (31). Although the different target antigen specificities of epratuzumab and rituximab may partly contribute to the different infusion characteristics, the different framework regions may also play an important role.

Second, we used a panel of cell lines to evaluate the ability of the MAbs to kill NHL cells. Cell lines were included as a variable because our experience has shown that various cell lines respond differently to immunotherapy. We observed differences in the ability of the MAbs to inhibit proliferation, as well as induce apoptosis, ADCC, and CMC. These results were not directly related to antigen density. This is consistent with the observations of others with anti-CD20 MAbs (32) as well as other anti-B-cell MAbs (16). Nagy *et al.* (16) reported a nonlinear correlation between killing efficiency with anti-HLA-DR MAbs and the level of HLA-DR antigen expression. Chan *et al.*

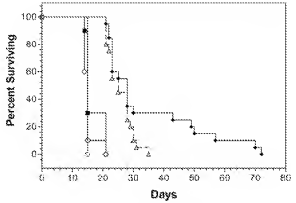

Fig. 9 Combination therapy IMMU-106 and epratuzumab in Raji-bearing SCID mice. Monoclonal antibodies were administered to SCID mice 2 times/week at 50 μg/injection. Monoclonal antibody injections were initiated 1 day after i.v. injection of Raji cells. Results shown include combined data from animals treated on two dates. The first included animals treated with hMN-14 (n = 10), IMMU-106 (n = 10), epratuzumab (n = 10), and IMMU-106+epratuzumab (n = 10). The second included animals treated with IMMU-106 (n = 10), IMMU-106+epratuzumab (n = 10), and control untreated mice (n = 9). ▲, IMMU-106; ◆, IMMU-106+Epratuzumab; ◇, Epratuzumab; ■, hMN-14; ○, untreated.

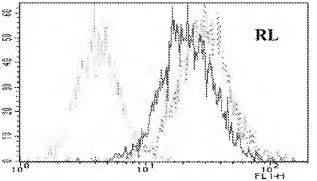

Fig. 10 Up-regulation of CD22 by anti-CD20 (IMMU-106) in RL cells. Cell lines were incubated ~17 h with a saturating concentration of IMMU-106 or no monoclonal antibody (MAb). The CD22 and CD20 expression was then measured by flow cytometry using FITC-RFB4, an anti-CD22 MAb that blocks epratuzumab binding, and FITC-B1, which blocks IMMU-106 binding. CD8 expression was also measured as a negative control (FITC-anti-Leu-2a). RL cells stained with FITC-RFB4 either without MAb pretreatment (*purple line*) or after pretreatment with IMMU-106 (*green line*) are shown in comparison to the control untreated cells stained with FITC-anti-Leu-2a (*red line*). FITC-B1 staining is not shown.

(32) observed differences in the effects of anti-CD20 MAbs on a range of cell lines by various apoptotic and clonogenic assays. By analyzing the differences between cell lines, these authors concluded that apoptosis through CD20 was dependent on the nature of MAb binding and correlated with the extent of homotypic cell adhesion induced. In addition, they concluded that the extent of apoptosis was independent of translocation to Triton X-100 insoluble rafts, and that CD20 can evoke apoptosis without involvement of mitochondria and caspases. Control of sensitivity to CD20-induced apoptosis remains unclear; it is likely that signaling or effector molecules are missing or improperly regulated in insensitive tumor cell lines. These observations highlight the importance of studying a number of cell lines before drawing a conclusion on clinical relevance, as well as demonstrating how correlating mechanistic assays with efficacy observations can shed light on innate and/or acquired resistance to antibody therapy.

Third, we examined the effects of combining anti-CD20 and anti-CD22 treatments. Epratuzumab, and the anti-CD20 MAbs IMMU-106 and rituximab, recognize distinct antigens and achieve their efficacy through different mechanisms. Anti-CD20 MAbs, including rituximab, have been shown to induce ADCC and CMC in tumor target cells (2–5, 33). In addition, evidence from *in vitro* studies, animal tumor models, and clinical trials suggest that the tumoricidal effect of naked anti-CD20 MAbs does not occur solely by these mechanisms. Antibody binding to CD20 has been shown to inhibit cell cycle progression after mitogen stimulation (34); inhibit B-lymphocyte differentiation (35); inhibit EBV and pokeweed mitogen-induced immunoglobulin secretion (34, 35); and generate a transmembrane signal that results in enhanced phosphorylation of the molecule (36), increase of tyrosine-kinase activity (37), and induction of c-myc oncogene expression (38). Shan *et al.* (6) demonstrated that extensive cross-linking of CD20 with murine anti-CD20 MAbs in the presence of either goat antimouse IgG or Fc receptor-expressing cells directly inhibits B-cell proliferation, induces nuclear DNA fragmentation, and leads to cell death by apoptosis. Apoptotic effects can be inhibited by chelation of intracellular or extracellular calcium ions. These results suggest that ligation of CD20 *in vivo* by MAbs in the presence of Fc receptor-expressing cells may initiate signal transduction events, increase calcium ion levels, and lead to apoptosis.

CD22 functions as an adhesion receptor for B cells, T cells, monocytes, neutrophils, and RBCs (39), and is involved in signal transduction, modulating B-cell antigen receptor-mediated signal transduction (40). Ligation of CD22 with MAbs that block the ligand-binding site triggers rapid tyrosine phosphorylation of CD22 and primary B-cell proliferation (41). In contrast to the binding of the anti-CD22 MAb, HB22.23, epratuzumab does not block the ligand-binding site on CD22 (42). However, ligation of CD22 with epratuzumab does cause rapid internalization of the MAb and also induces phosphorylation of the CD22 cytoplasmic tail (42). The rapid internalization of this MAb into NHL cells has facilitated its use for the delivery of toxins within the cells (43, 44). A key role for CD22 in B-cell function is also suggested by studies showing that CD22-deficient mice have a shorter life span, a reduced number of mature B cells, a chronic exaggerated antibody response to antigen, and development of elevated levels of autoantibodies (45). Many of these functions can be modulated by epratuzumab through CD22 phosphorylation and CD22 internalization (42).

In clinical studies epratuzumab has shown antitumor responses as an unlabeled agent (30) and in radioimmunotherapy applications (31, 46, 47). Unlabeled, epratuzumab has shown evidence of antitumor activity in patients with recurrent NHL, producing responses, including complete responses, in patients with follicular and diffuse large B-cell histologies. In a dose escalation study examining the safety, efficacy, and pharmacokinetics of epratuzumab in patients with recurrent indolent NHL, Leonard *et al.* (30) administered 120-1000 mg/m^2 over 30–60 min for four weekly treatments. These doses were well tolerated with no dose-limiting toxicities and had clinical activity. A 43% objective response rate was observed in follicular NHL patients receiving 360 mg/m^2/week, similar to results observed using rituximab. Greater than 95% of the infusions were completed in ~1 h. The fact that epratuzumab does not activate complement and, thus, produces a less-dramatic depletion of B cells may contribute to the excellent infusion tolerability. In addition, these dosing regimens resulted in an extended half-life of 23 days, compared with ~10 days with rituximab (30).

Thus, the combination of epratuzumab with an anti-CD20 MAb may be beneficial, yielding additive or synergistic activities. Preliminary findings in a murine model (48) and in patients (49) indicate that the combination of rituximab and epratuzumab is well tolerated and may result in improved antilymphoma activity *versus* the single agents. Clinically, the overall response rate of epratuzumab combined with rituximab in indolent, follicular NHL was reported to be similar to that of rituximab alone, but a higher complete response rate was found (49). Thus, it would seem that these two antigen targets overlap in terms of responsiveness in this tumor type, with the combination only improving the magnitude of the rituximab response in contrast to more patients responding when epratuzumab is added. This implies that the combination is synergistic in those patients having both target antigens and responding to either agent.

As reported here, we found that the combination of IMMU-106 and epratuzumab appears to be more effective than either MAb alone in the SU-DHL-6 tumor cell line. *In vitro*, the combination of these two MAbs increased inhibition of proliferation from 53% for IMMU-106 alone to 83% in cultured SU-DHL-6 cells. *In vivo*, in SCID mice bearing disseminated Raji cells, prolonged survival was observed in 30% of the mice given IMMU-106 and epratuzumab, compared with IMMU-106 monotherapy. These results are consistent with the clinical observations and may be explained partially by the up-regulation of CD22 expression after treatment of NHL cells with CD20 MAb, implying that higher antigen expression may contribute to more effective therapy. It is not clear why cross-linking of CD20 increases CD22 expression and not *vice versa*. Additive or synergistic results on signaling events initiated by the anti-CD20 and -CD22 MAbs may be the cause of the increased efficacy when the two agents are used in combination, although there may be little or no observed antiproliferative effects of the anti-CD22 MAb when given alone. Although there are many limitations to the use of xenografted NHL cell lines, especially because the SCID or nude mice do not have normal B cells that express the target human B-cell lineage antigens in question,

many of the observations made clinically can be reproduced in some of these models, such as the efficacy of naked CD20 MAbs as a monotherapy and in combination with epratuzumab shown in this article. The fact that the animal model reflects what has been seen in clinical studies encourages us to pursue the study of other variables in the preclinical setting, which would be impractical, if not impossible, to evaluate clinically.

In conclusion, the data shown here suggest that the mechanisms of cytotoxicity of IMMU-106, like rituximab, include direct apoptotic effects, as well as ADCC and complement-mediated cell lysis. It is expected that in humans, IMMU-106 should be at least as effective as rituximab and, due to its construction based on the framework of epratuzumab, it may exhibit different pharmacokinetic, toxicity, and therapy profiles. In addition, the results indicate that it may be possible to enhance efficacy by combination therapy comprised of anti-CD20 and other B-cell lineage targeting MAbs, such as epratuzumab, which supports current clinical studies of the combination of rituximab and epratuzumab in NHL therapy (49).

REFERENCES

1. Reff ME, Hariharan K, Braslawsky G. Future of monoclonal antibodies in the treatment of hematologic malignancies. Cancer Control 2002;9:152–66.

2. Golay J, Zaffaroni L, Baccan T. Biologic response of B lymphoma cells to anti-CD20 monoclonal antibody rituximab in vitro: CD55 and CD59 regulate complement-mediate cell lysis. Blood 2000;95:3900–8.

3. Harjunpaa A, Junnikkala J, Meri S. Rituximab (anti-CD20) therapy of B-cell lymphomas: direct complement killing is superior to cellular effector mechanisms. Scand J Immunol 2000;51:634–41.

4. Treon SP, Mitsiades C, Mitsiades N, et al. Tumor cell expression of CD59 is associated with resistance to CD20 serotherapy in patients with B-cell malignancies. J Immunother 2001;24:263–71.

5. Clynes RA, Towers TL, Presta LG, Ravetch JV. Inhibitory Fc receptors modulate in vivo cytoxicity against tumor targets. Nat Med 2000;6:443–6.

6. Shan D, Ledbetter JA, Press OW. Apoptosis of malignant human B cells by ligation with monoclonal antibodies. Blood 1998;91:1644–52.

7. Pedersen IM, Buhl AM, Klausen P, Geisler CH, Jurlander J. The chimeric anti-CD20 antibody rituximab induces apoptosis in B-cell chronic lymphocytic leukemia cells through a p38 mitogen activated protein-kinase-dependent mechanism. Blood 2002;99:1314–9.

8. Ghetie MA, Bright H, Vitetta ES. Homodimers but not monomers of Rituxan (chimeric anti-CD20) induce apoptosis in human B-lymphoma cells and synergize with a chemotherapeutic agent and an immunotoxin. Blood 2001;97:1392–8.

9. McLaughlin P, Grillo-Lopez AJ, Link BK, et al. Rituximab chimeric anti-CD20 monoclonal antibody therapy for relapsed indolent lymphoma: half of patients respond to a four dose treatment program. J Clin Oncol 1998;16:2825–33.

10. Davis TA, Grillo-Lopez AJ, White CA, et al. Rituximab anti-CD20 monoclonal antibody therapy in non-Hodgkin's lymphoma: safety and efficacy of retreatment. J Clin Oncol 2000;17:3135–43.

11. Maloney DG, Grilloop-Lopez AJ, White CA, et al. IDEC-C2B8 (Rituximab) anti-CD20 monoclonal antibody therapy in patients with relapsed low-grade non-Hodgkin's lymphoma. Blood 1997;90:2188–95.

12. Goldenberg DM, Horowitz JA, Sharkey RM, et al. Targeting, dosimetry, and radioimmunotherapy of B-cell lymphomas with iodine-131-labeled LL2 monoclonal antibody. J Clin Oncol 1991;9:548–64.

13. Younes A, Hariharan K, Allen RS, Leigh BR. Initial trials of anti-CD80 monoclonal antibody (Galiximab) therapy for patients with relapsed or refractory follicular lymphoma. Clin Lymphoma 2003;3:257–9.

14. Leonard JP, Link BK. Immunotherapy of non-Hodgkin's lymphoma with hLL2 (epratuzumab, an anti-CD22 monoclonal antibody) and Hu1D10 (apolizumab). Semin Oncol 2002;29:81–6.

15. Keating MJ, Flinn I, Jain V, et al. Therapeutic role of alemtuzumab (Campath-1H) in patients who have failed fludarabine: results of a large international study. Blood 2002;99:3554–61.

16. Nagy Z, Hubner B, Lohning C, et al. Fully human, HLA-DR-specific monoclonal antibodies efficiently induce programmed death of malignant lymphoid cells. Nat Med 2002;8:801–7.

17. Ochakovskaya R, Osorio L, Goldenberg DM, Mattes MJ. Therapy of disseminated B-cell lymphoma xenografts in severe combined immunodeficient mice with an anti-CD74 antibody conjugated with (111)indium, (67)gallium, or (90)yttrium. Clin Cancer Res 2001;7:1505–10.

18. Coleman M, Goldenberg DM, Siegel AB, et al. Epratuzumab: targeting B-cell malignancies through CD22. Clin Cancer Res 2003;9:3991s–4s.

19. Hekman A, Honselaar A, Vuist W, et al. Initial experience with treatment of human B cell lymphoma with anti-CD19 monoclonal antibody. Cancer Immunol Immunother 1991;32:364–72.

20. Leung SO, Goldenberg DM, Dion AS, et al. Construction and characterization of a humanized, internalizing, B-cell (CD22)-specific, leukemia/lymphoma antibody, LL2. Molecular Immunol 1995;32:1416–27.

21. Losman MJ, Hansen HJ, Dworak H, et al. Generation of a high-producing clone of a humanized anti-B-cell lymphoma monoclonal antibody (hLL2). Cancer 1997;80:2660–6.

22. Leung SO, Shevitz J, Pellegrini MC, et al. Chimerization of LL2, a rapidly internalizing antibody specific for B cell lymphoma. Hybridoma 1994;13:469–76.

23. Sharkey RM, Juweid M, Shevitz J, et al. Evaluation of a complementarity-determining region-grafted (humanized) anti-carcinoembryonic antigen monoclonal antibody in preclinical and clinical studies. Cancer Res 1995;55:5935s–45s.

24. Trucco M, de Petris S, Garotta G, Ceppellini R. Quantitative analysis of cell surface HLA structures by means of monoclonal antibodies. Human Immunol 1980;3:233–43.

25. Lindmo T, Boven E, Cuttitta F, Fedorko J, Bunn PA Jr Determination of the immunoreactive fraction of radiolabeled monoclonal antibodies by linear extrapolation to binding at infinite antigen excess. J Immunol Meth 1984;72:77–89.

26. McConahey PJ, Dixon FJ. A method of trace iodination of proteins for immunologic studies. Int Arch Allergy 1966;29:185–9.

27. Stein R, Chen S, Grossman W, Goldenberg DM. Human lung carcinoma monoclonal antibody specific for the Thomsen-Friedenreich antigen. Cancer Res 1989;49:32–7.

28. Nicoletti I, Migliorati G, Pagliacci MC, Grignani F, Riccardi C. A rapid and simple method for measuring thymocyte apoptosis by propidium iodide staining and flow cytometry. J Immunol Methods 1991;139:271–9.

29. Cardarelli PM, Quinn M, Buckman D, et al. Binding to CD20 by anti-B1 antibody or F(ab')$_2$ is sufficient for induction of apoptosis in B-cell lines. Cancer Immunol Immunother 2002;51:15–24.

30. Leonard JP, Coleman M, Ketas JC, et al. Phase I/II trial of epratuzumab (humanized anti-CD22 antibody) in indolent non-Hodgkin's lymphoma. J Clin Oncol 2003;21:3051–9.

31. Lindén O, Cavallin-Ståhl E, Strand, S-E, et al. 90-Yttrium-epratuzumab in patients with B-cell lymphoma failing chemotherapy, using a dose fractionation schedule. Cancer Biother Radiopharm 2002;17:490.

32. Chan HT, Hughes D, French RR, et al. CD20-induced lymphoma cell death is independent of both caspases and its redistribution into triton X-100 insoluble membrane rafts. Cancer Res 2003;63:5480–9.

33. Reff ME, Carner K, Chambers KS, et al. Depletion of B cells in vivo by a chimeric mouse human monoclonal antibody to CD20. Blood 1994;83:435–45.

34. Tedder TF, Forsgren A, Boyd AW, Nadler LM, Schlossman SF. Antibodies reactive with the B1 molecule inhibit cell cycle progression but not activation of human B lymphocytes. Eur J Immunol 1986;16:881–7.

35. Golay JT, Crawford DH. Pathways of human B-lymphocyte activation blocked by B-cell specific monoclonal antibodies. Immunology 1987;62:279–84.

36. Tedder TF, Schlossman SF. Phosphorylation of the B1 (CD20) molecule by normal and malignant human B lymphocytes. J Biol Chem 1988;263:10009–15.

37. Kansas GS, Tedder TF. Transmembrane signals generated through MHC class II, CD19, CD20, CD39, and CD40 antigens induce LFA-1-dependent and independent adhesion in human B cells through a tyrosine kinase-dependent pathway. J Immunol 1991;147:4094–102.

38. Smeland EB, Beiske K, Ek B, et al. Regulation of c-myc transcription and protein expression during activation of normal human B cells. Exp Cell Res 1987;172:101–9.

39. Kehrl CD20 Workshop Panel report. In: Schlossman SF, Boumsell L, Gilks W, Harlan JM, Kishimoto T, Morimoto C, Ritz J, Shaw S, Silverstein R, Springer T, Tedder TF, and Todd RF, editors. Leukocyte Typing V. White cell differentiation antigens. proceedings of the fifth International Workshop and Conference., Vol. 1. New York: Oxford University Press, 1995. p. 523–525.

40. Peaker CJ, Neuberger MS. Association of CD22 with the B cell antigen receptor. Eur J Immunol 1993;23:1358–63.

41. Tuscano JM, Riva A, Toscano SN, Tedder TF, Kehrl JH. CD22 Cross-linking generates B-cell antigen receptor-independent signals that activate the JNK/SAPK signaling cascade. Blood 1999;94:1382–92.

42. Carnahan J, Wang P, Kendall R, et al. Epratuzumab, a humanized monoclonal antibody targeting CD22: characteriazation of in vitro properties. Clin Cancer Res 2003;9:3982s–90s.

43. Kreitman RJ, Hansen HJ, Jones AL, FitzGerald DJ, Goldenberg DM, Pastan I. Pseudomonas exotoxin-based immunotoxins containing the antibody LL2 or LL2-Fab' induce regression of subcutaneous human B-cell lymphoma in mice. Cancer Res 1993;53:819–25.

44. Newton DL, Hansen HJ, Mikulski SM, Goldenberg DM, Rybak SM. Potent and specific antitumor effects of an anti-CD22-targeted cytotoxic ribonuclease: potential for the treatment of non-Hodgkin lymphoma. Blood 2001;97:528–35.

45. Otipoby KL, Andersson KB, Draves KE, et al. CD22 regulates thymus-independent responses and the lifespan of B cells. Nature 1996; 384:634–7.

46. Juweid ME, Stadtmauer E, Hajjar G, et al. Pharmacokinetics, dosimetry, and initial therapeutic results with ^{131}I and ^{111}In-/^{90}Y-labeled humanized LL2 anti-CD22 monoclonal antibody in patients with relapsed, refractory non-Hodgkin's lymphoma. Clin Cancer Res 1999;5: 3292s–303s.

47. Griffiths GL, Govindan SV, Sharkey RM, Fisher DR, Goldenberg DM. ^{90}Y-DOTA-hLL2: an agent for radioimmunotherapy of non-Hodgkin's lymphoma. J Nucl Med 2003;44:77–84.

48. Hernandez-Ilizaliturri F, Gada P, Repasky E, Czuczman M. Enhancement in anti-tumor activity of rituximab when combined with epratuzumab or apolizumab (Hu1D10) in a B-cell lymphoma severe combined deficiency (SCID) mouse model. Blood 2002;100:591.

49. Leonard JP, Coleman M, Matthews JC, et al. Epratuzumab (anti-CD22) and rituximab (anti-CD20) combination immunotherapy for non-Hodgkin's lymphoma: Preliminary response data. Proc Am Soc Clin Oncol 2002;21:1060.